LES-DPS OF THE EFFECT OF WALL ROUGHNESS ON DISPERSED-PHASE TRANSPORT IN PARTICLE-LADEN TURBULENT CHANNEL FLOW

Kyle D. Squires
Mechanical and Aerospace Engineering Department,
Arizona State University
Tempe, Arizona 85287-6106, USA
squires@asu.edu

Olivier Simonin
Institut de Mécanique des Fluides,
UMR 5502 CNRS/INPT/UPS
31400 Toulouse, France
simonin@imft.fr

ABSTRACT

The influence of wall roughness on the properties of particle-laden turbulent channel flow is investigated using Large Eddy Simulation (LES) for the fluid and Discrete Particle Simulation (DPS) for the particulate phase. The influence of wall roughness is treated stochastically following the approach of Sommerfeld (1992) in which the impact angle of the particle is comprised of the particle trajectory angle and a stochastic component due to wall roughness.

Particle-wall collisions are elastic and for each of the three Stokes numbers considered computations are performed with standard deviation of the distribution of "wall roughness angles" of 0 (smooth wall), 2.5 and 5 degrees. Simulation results show that for a given wall roughness angle and particle Stokes number the most pronounced effect of roughness is on the wall-normal component of the particle velocity, which can be substantially increased by roughness. While the streamwise particle velocity variance is also increased by roughness, the spanwise component of the particle velocity variance exhibits relatively little sensitivity to surface roughness. Turbulent transport of the particle velocity variance can be strongly affected by roughness and can also provide a mechanism for transport of the particle velocity variance across the channel.

INTRODUCTION

Turbulent gas flows containing dilute suspensions of solid particles are complex and pose many technologically challenging and scientifically relevant questions. For the practical applications in which particle-laden turbulent flows are encountered, statistical models that require substantial empirical input will continue to form the basis for engineering prediction. The fundamental knowledge base that is crucial for guiding the development of models for applications is not sufficiently developed. This is in large part due to the difficulty in measuring quantities in the reference frame most naturally suited for analysis, i.e., the Lagrangian reference frame attached to a particle. This complicates experiments and motivates the application of numerical simulations that enable detailed investigation of many of the processes governing turbulent two-phase flows.

For dilute, gas-solid turbulent flows, numerical techniques that resolve some or all of the underlying eddy motions of the carrier-phase have an important role in advancing fundamental understanding of the various interactions important to accurately predicting dispersed-phase properties. These numerical approaches – Direct Numerical Simulation (DNS) and Large Eddy Simulation (LES) – together with Discrete Particle Simulation (DPS) have been applied in several previous investigations aimed at understanding particle transport by turbulence, particle-particle collisions, and turbulence modulation by momentum exchange with heavy particles (e.g., see Laviéville *et al.* 1995, Wang and Squires 1996, Yamamoto *et al.* 2001).

Less investigated than the effects cited above using techniques such as DNS and LES, and the topic of the present effort, is the influence of wall roughness on particulate-phase transport. Experimental investigations have shown that wall roughness can strongly alter particle motion and in turn cause measurable changes to the overall flow properties. Sommerfeld and Huber (1999) showed that wall roughness altered the rebound behavior of particles in a horizontal channel which, on average, resulted in a re-dispersion of the particles as well as a lowering of the settling rate as compared to measurements in smooth-wall configurations. Kussin and Sommerfeld (2002) obtained measurements of gas-solid, horizontal channel flow using spherical beads with diameters ranging from 60 microns to 1 mm. A focus of this work was variation of wall roughness by changing the wall plates. Their measurements showed that wall roughness enhanced the particle fluctuating velocity due to the irregular bouncing of the particle with a rough wall and lead to a more uniform distribution of particles across the channel.

In general, wall roughness introduces an effect analogous to that produced by particle-particle collisions: amplification of wall-normal (or, in a pipe, radial) particle velocity fluctuations that can substantially change the transport characteristics of the particles and cause large changes in other flow properties, e.g., the overall pressure drop of a gas-solid mixture. Sommerfeld and Huber (1999) used their experiments to measure parameters for a wall-collision model employed in Lagrangian approaches for gas-particle flows (e.g., see Sommerfeld 2003). As described below, a similar approach to incorporating the

effect of wall roughness into the computations is employed in the present study.

As summarized in the next section, the computational approach is based on LES of fully-developed turbulent channel flow combined with Discrete Particle Simulation (DPS) of the dispersed phase. The particle equation of motion and parameter space of the present investigations are presented and followed by statistical descriptors of particulate-phase motion used to assess roughness effects. A summary of the work and perspectives gained are then outlined.

APPROACH

LES of turbulent channel flow

The flow under consideration is a vertical, fully-developed turbulent channel flow (i.e., without gravitational settling on either of the channel walls). The numerical approach employs Large Eddy Simulation (LES) of the carrier-phase flow and Discrete Particle Simulation (DPS) for prediction of dispersed phase transport. The fluid flow is maintained at constant mass flux corresponding to a target Reynolds number $Re_\tau = 180$ based on the friction velocity u_τ and channel halfwidth δ. The dimensions of the channel are $4\pi\delta$ in the streamwise (x or x_1), $4\pi\delta/3$ in the spanwise (z or x_3), and 2δ in the wall-normal (y or x_2) directions. Periodic boundary conditions are applied to the dependent variables in the streamwise and spanwise dimensions and no-slip boundary conditions to the velocity at the channel walls. The subgrid-scale stress arising from the filtering of the Navier-Stokes equations is closed using a Smagorinsky eddy viscosity model.

The equations governing the fluid flow are solved using a fractional step method. The fluid-flow solutions are resolved on a staggered mesh comprised of $64 \times 65 \times 64$ cells in the x, y, and z directions, respectively. The grid spacings in the streamwise and spanwise directions are uniform with corresponding spacings in viscous units of $\Delta x^+ = 35$ and $\Delta z^+ = 12$. Spatial derivatives are approximated using second-order accurate central differences. The Poisson equation formulated for the pressure variable that is used to obtain a divergence-free velocity field is solved using fast transforms in the streamwise and spanwise direction, resulting in a series of tri-diagonal matrices that are efficiently inverted in the direction normal to the solid walls. The wall-normal mesh is clustered near the solid surfaces and stretched away from the wall using a hyperbolic tangent function. The discretized system is advanced in time using an implicit/explicit time advance (Crank-Nicholson and second-order Adams-Bashforth).

Dispersed Particle Simulation

The focus of the current work is on dilute gas-solid flows in the limit of one-way coupling for which there is no modification of the carrier phase flow due to the presence of the dispersed phase. In addition, effects of inter-particle collisions are not included in the present simulations. The particle diameter d_p is assumed small compared to the smallest turbulent lengthscales of the undisturbed fluid flow. The particle density is much larger than that of the fluid phase, ($\rho_p \gg \rho_f$, where ρ_f is the fluid density and the ρ_p is the particle density. Owing to the large density ratio, the particle response time is large compared to the Kolmogorov timescale of the undisturbed flow.

Table 1: Particle parameters for turbulent channel flow, $Re_\tau = 180$. The particle diameter for each case is one viscous unit, $d_p^+ = 1$. The time constant in viscous units, $\tau_{ps}^+ = StRe_\tau$.

ρ_p/ρ_f	527	2106	8424
St	0.1625	0.65	2.60
τ_{ps}^+	29	117	468

For the dilute regimes under consideration, the force induced by the surrounding fluid flow on the particles reduces to the drag. The equation of motion for a single particle is written as,

$$\frac{dv_{p,i}}{dt} = -\frac{3}{4}\frac{\rho_f}{\rho_p}\frac{C_D}{d_p}|\vec{v}_r|v_{r,i}\,, \tag{1}$$

where $v_{p,i}$ is the i^{th} component of the particle velocity and $v_{r,i}$ is the particle relative velocity,

$$v_{r,i} = v_{p,i} - \widetilde{u}_{f,i}\,, \tag{2}$$

$$C_D = \frac{24}{Re_p}(1 + 0.15Re_p^{0.687})\,, \qquad Re_p = \frac{|\vec{v}_r|d_p}{\nu_f}\,. \tag{3}$$

Simulations are performed for three particle Stokes numbers, $St = \tau_{ps}/(\delta/u_\tau)$, where τ_{ps} is the Stokes relaxation timescale of the particle. For all simulations the particle diameter was specified as one viscous unit and therefore the variation in the Stokes number is achieved via a variation in the density ratio, as summarized in Table 1. The particle response times are chosen so that the lightest particles ($St = 0.1625$) follow reasonably well the turbulent fluctuations in the carrier phase, while for the largest $St = 2.60$ the particles are largely unaffected by the carrier flow.

Properties of the dispersed phase are obtained via Lagrangian tracking of 1×10^5 particles, corresponding to an average number density of 950 particles per unit volume, equivalent to a dispersed-phase volume fraction of 8.5×10^{-5}. The particle equation of motion (1) is integrated in time using second-order Adams-Bashforth. Third-order Lagrange polynomials are used to interpolate the fluid velocity to the particle position. Particle displacements are also integrated using the second-order Adams-Bashforth method. For particles that move out of the channel in the streamwise or spanwise directions, periodic boundary conditions are used to reintroduce them into the computational domain.

In this work, the fluid flow is not influenced by momentum exchange with the particles and the (undisturbed) fluid velocity $\widetilde{u}_{f,i}$, required in (2), is the value interpolated to the particle position that is computed in the LES, representing the spatially-filtered (volume averaged) solution of the Navier-Stokes equations. The influence of subgrid-scale transport on particle motion is not considered, which should be a reasonable assumption given the filtering by particle inertia of the smaller-scale, high-frequency components of the subgrid fluid velocity (e.g., see Yamamoto *et al.* 2001). However, the neglect of subgrid transport restricts the parameter range of the current calculations, e.g., to moderate Reynolds numbers for which there is a relatively weak effect of the unresolved motions on the resolved scales. In other regimes, such as very

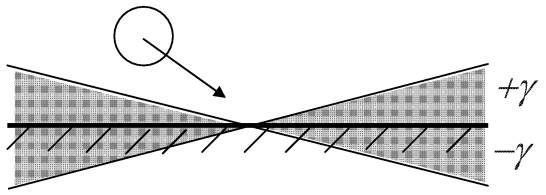

Figure 1: Schematic illustrating particle collision with "virtual wall" in which particle collides with a wall given a random inclination. Wall roughness angles are sampled from a Gaussian distribution that is characterized by its standard deviation γ'.

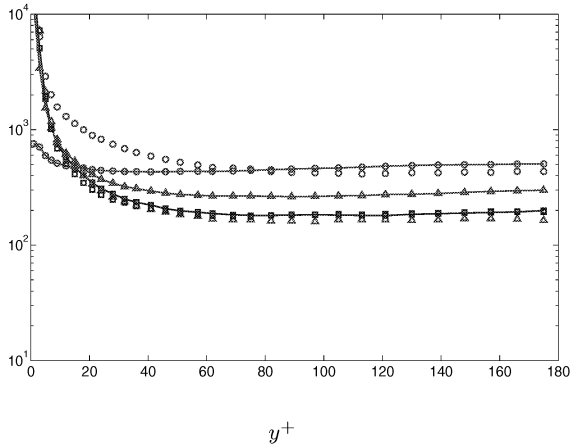

Figure 2: Number density. Rough-wall results with $\gamma' = 5°$ shown using symbols and lines; smooth-wall ($\gamma' = 0°$) cases shown using symbols only. □ $St = 0.1625$; △ $St = 0.65$; ○ $St = 2.60$.

small particle response times, the errors introduced by transporting the particulate phase by a filtered fluid velocity should be significant and will require models of the subgrid velocities on particle motion.

Particle-wall collisions are elastic with wall roughness simulated using a statistical treatment. A particle collides with a "virtual wall" which has a randomly distributed inclination with respect to the plane, smooth wall (c.f., Figure 1). The "wall roughness angle" is denoted γ in Figure 1 and is sampled from a Gaussian distribution. The stochastic treatment is very similar to that employed in Sommerfeld (2003) and other related references. Three values of the standard deviation, γ', of the distribution of wall roughness angles are considered: 0° (smooth wall), 2.5°, and 5°. These values are within the range of the measurements from Sommerfeld and Huber (1999) used to develop and validate roughness models for Lagrangian approaches.

RESULTS

Mean flow

Shown in Figure 2 is the wall-normal profile of the mean particle number density for each Stokes number and from a smooth-wall case ($\gamma' = 0°$) and rough-wall case with $\gamma' = 5°$.

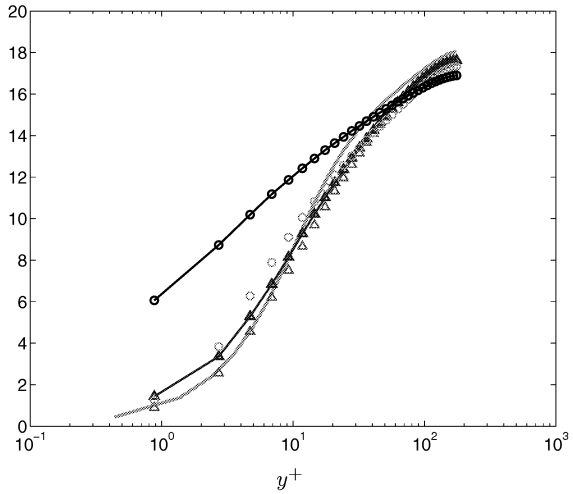

Figure 3: Streamwise mean velocity. Rough-wall results with $\gamma' = 2.5°$ shown using symbols and lines; smooth-wall ($\gamma' = 0°$) cases shown using symbols only. ——— fluid; △ $St = 0.65$; ○ $St = 2.60$.

The figure shows that for particle-wall collisions with a smooth wall the number density distribution indicates that there is the characteristic peak at the wall as typically observed in channel flow in which particle-particle collisions are not considered and for which there is a specular reflection of the particle on the wall (e.g., see Yamamoto *et al.* 2001). As shown in the figure, the most significant non-uniformity in the wall-normal profiles is observed for the lower Stokes numbers, $St = 0.1625, 0.65$.

Figure 2 also shows that, compared to the smooth-wall profiles, for the rough wall with $\gamma' = 5°$ the number density profile exhibits the largest changes for the larger Stokes numbers. For the lightest particles, $St = 0.1625$, there are insignificant changes in the number density and in other statistics not shown here. For the larger Stokes numbers the influence of wall roughness becomes more apparent with a significantly lower near-wall number density, especially for $St = 2.60$.

The effect of wall roughness on the streamwise mean particle velocity is shown in Figure 3 for $St = 0.65$ and $St = 2.60$ at roughness angles of 0 and 2.5 degrees. Also shown in the figure is the profile of the mean fluid velocity (on the grid, i.e., not following particles). For the smooth-wall cases (symbols-only in the figure) the mean slip between the particles and fluid is small and, consequently, the mean velocity of the particles is close to that of the fluid. Analogous to the more uniform profiles achieved in the number density in Figure 2, for cases in which particles collide with rough walls, Figure 3 shows that the particle mean velocity profile becomes more uniform across the channel, this effect is the most apparent for the largest Stokes number, $St = 2.60$, where the velocity is not only more uniform for the rough-wall case but also slips relative to the wall, which is compatible with the elastic bouncing of the particles on the wall as considered in the current simulations.

The mean number density and mean streamwise velocity in Figure 2 and Figure 3 show effects of wall roughness that appear similar to those produced by inter-particle collisions in which the redistribution of particle kinetic energy by particle-particle collisions provides a mechanism for increasing cross-stream (radial) transport, and also leads to more uniform

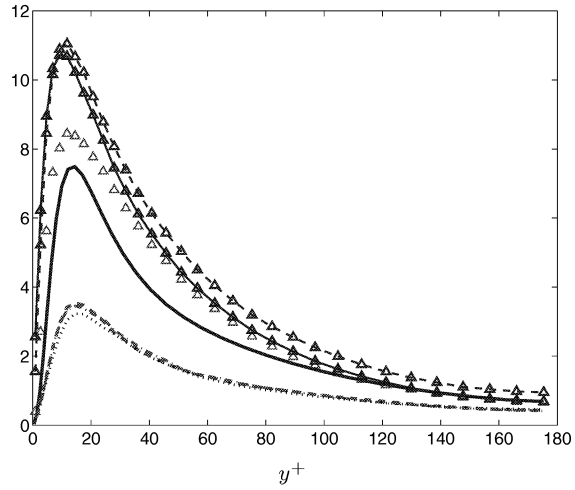

Figure 4: Influence of roughness on streamwise velocity variance, $St = 0.65$. ——— fluid; △ smooth wall; △——△ $\gamma' = 2.5°$; △--△ $\gamma' = 5°$; —·— fluid-particle correlation for smooth wall; - - - - fluid-particle correlation for $\gamma' = 2.5°$; ····· fluid-particle correlation for $\gamma' = 5°$.

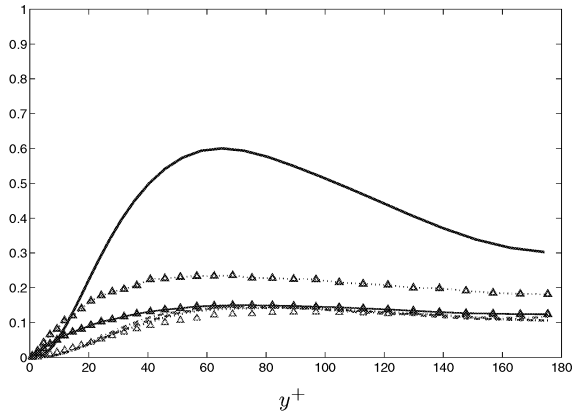

Figure 5: Influence of roughness on wall-normal velocity variance, $St = 0.65$. ——— fluid; △ smooth wall; △——△ $\gamma' = 2.5°$; △·····△ $\gamma' = 5°$; —·— fluid-particle correlation for smooth wall; - - - - fluid-particle correlation for $\gamma' = 2.5°$; ····· fluid-particle correlation for $\gamma' = 5°$.

number density distributions and particle mean velocities.

Influence of wall roughness on particle velocity variance

The influence of wall roughness on the particle velocity variance for $St = 0.65$ is shown in Figures 4, 5, and 6 for the streamwise, wall-normal, and spanwise directions, respectively. The calculations shown in these figures are for the intermediate Stokes number, $St = 0.65$, and are representative of the other Stokes numbers not shown here. Plotted in each figure is the particle velocity variance for the three roughness angles in addition to the fluid variance as well as curves corresponding to the fluid-particle velocity correlation, $\langle \widetilde{u}'_{f,\alpha} v'_{p,\alpha} \rangle_p$ where $\langle \cdot \rangle_p$ denotes an average over the particulate phase. Note that the curves corresponding to $\langle \widetilde{u}'_{f,\alpha} v'_{p,\alpha} \rangle_p$ are obtained for each wall roughness case.

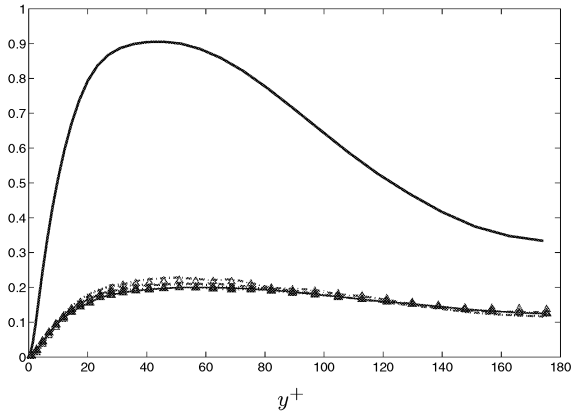

Figure 6: Influence of roughness on spanwise velocity variance, $St = 0.65$. ——— fluid; △ smooth wall; △——△ $\gamma' = 2.5°$; △--△ $\gamma' = 5°$; —·— fluid-particle correlation for smooth wall; - - - - fluid-particle correlation for $\gamma' = 2.5°$; ····· fluid-particle correlation for $\gamma' = 5°$.

The general effects of wall roughness emerging from Figures 4-6 is an increase of the wall-normal and streamwise particle velocity variance, with the largest effects of roughness on the wall-normal variance, and then with negligible effects of wall roughness on the spanwise particle velocity variance. Figure 4 shows that for the smooth-wall case ($\gamma' = 0°$), the particle velocity fluctuations for $St = 0.65$ exceed the fluid levels near the wall and are also substantially larger than the fluid-particle velocity variance. As shown by Simonin *et al.* (1995) and Wang and Squires (1996), this feature arises due to the production of the streamwise particle velocity variance, which is enlarged by the gradients in both the mean particle and fluid velocities and can in fact become larger than the corresponding value for the fluid, as shown in the figure. While the streamwise particle velocity variance is comparable (larger) than that for the fluid, Figures 5 and 6 show that the wall-normal and spanwise velocity variances for the smooth-wall case ($\gamma' = 0°$) are substantially smaller than that of the corresponding levels in the fluid. This is an intuitive effect of particle inertia which results in very large anisotropy of the particle velocity fluctuations in the smooth-wall case. Figures 5 and 6 also show that the particle wall-normal and spanwise velocity variances are in good agreement with the corresponding profiles of the fluid-particle velocity correlations, indicative of the fact that the the particle fluctuating velocities in these directions are controlled by the drag force, i.e., effects of turbulent dispersion (triple correlation transport) are not substantial and there is no direct influence of mean shear on these velocity fluctuations. Thus, particle fluctuating motion in these directions is at equilibrium with the local turbulent fluid flow.

Figure 5 also shows that for $\gamma' = 2.5°$ the wall-normal particle velocity variance is tangibly larger than the smooth-wall profile in the near-wall region (for values of y^+ less than about 50) and slightly larger than the smooth-wall profile to approximately $y^+ = 100$. With further increases in roughness, to $\gamma' = 5°$, Figure 5 shows that the wall-normal particle velocity variance is larger than the smooth-wall profile throughout the channel, showing that the effects of roughness on the particle fluctuating motion have permeated throughout the flow.

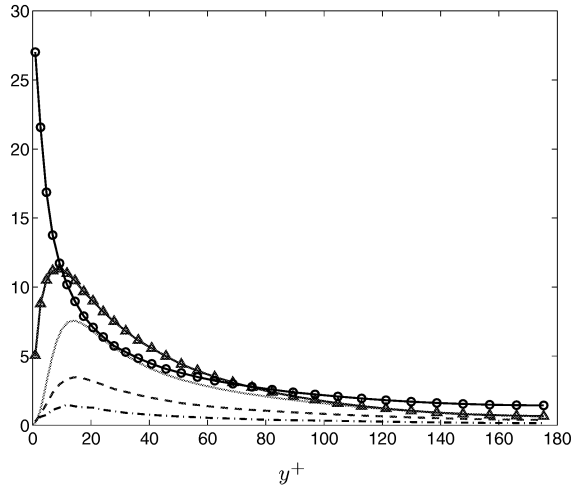

Figure 7: Influence of Stokes number on the streamwise velocity variance, $\gamma = 2.5°$. ——— fluid; △——△ $St = 0.65$; o——o $St = 2.60$; - - - - fluid-particle correlation for $St = 0.65$; —·— fluid-particle correlation for $St = 2.60$.

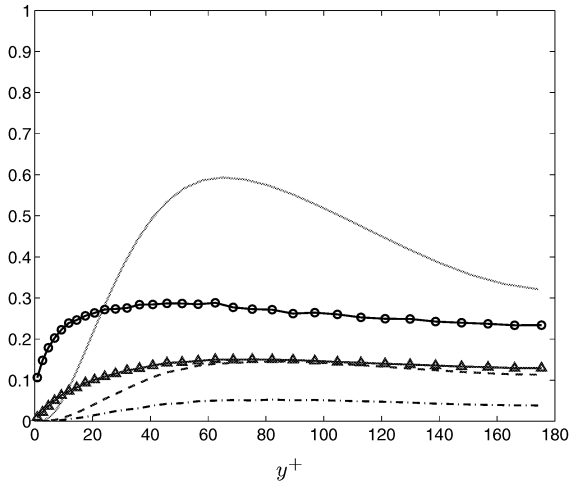

Figure 8: Influence of Stokes number on the wall-normal velocity variance, $\gamma = 2.5°$. ——— fluid; △——△ $St = 0.65$; o——o $St = 2.60$; - - - - fluid-particle correlation for $St = 0.65$; —·— fluid-particle correlation for $St = 2.60$.

Though not large, in the very near wall region, for y^+ smaller than about 10, Figure 5 shows that the particle variance is slightly larger than the fluid value. Also apparent from the figure is that the wall-normal particle velocity fluctuations are no longer at equilibrium with the local turbulent fluid flow, as evidenced by the discrepancy between the particle velocity variance and fluid-particle velocity correlation.

While Figure 5 shows that there is a relatively large increase with roughness in the wall-normal particle velocity fluctuations, Figure 4 shows that the streamwise velocity variance exhibits less sensitivity to increases in the roughness angle from 2.5° to 5°, indicative of a less efficient mechanism compared to that responsible for elevating the wall-normal particle velocity variance. As shown in Figure 6, the influence of wall roughness on the spanwise particle velocity variance is negligible with good agreement between the particle velocity variance and fluid-particle velocity correlation for all roughness angles. Also apparent in Figure 4 and Figure 5, while wall roughness can have strong effects on the particle velocity fluctuations, the fluid-particle correlations are virtually unchanged.

Influence of Stokes number on particle velocity variance

The effect of changes to the particle Stokes number on the particle velocity fluctuations for a given roughness angle are shown in Figures 7-9. The results in these figures are for a roughness angle of 2.5° and are representative of the effects observed for the larger angle $\gamma' = 5°$. Analogous to Figures 4-6, shown in Figures 7-9 are the profiles of the fluid velocity variance on the grid and fluid-particle velocity correlations for each Stokes number.

Each of Figures 7-9 show that the fluid-particle velocity correlation is decreased with increasing particle inertia and, as also observed previously for $St = 0.65$, the wall-parallel velocity variances (wall-normal and spanwise) for $St = 2.60$ are in good agreement with the corresponding components of the fluid-particle velocity correlation for the smooth-wall case, $\gamma = 0°$.

Figure 8 shows that the wall-normal particle velocity variance for $St = 2.60$ and $\gamma' = 2.5°$ is larger than the same curve for $St = 0.65$ and also substantially larger than the corresponding value of the fluid-particle velocity correlation (and therefore strongly above the particle velocity variance for the smooth-wall case). Figure 8, which shows the streamwise velocity variance, illustrates that for $St = 2.60$ the near-wall behavior is rather different than observed for $St = 0.65$, with a large increase in the variance at the wall. Figure 9 shows that the spanwise variance for $St = 2.60$ is essentially unchanged (except very close to the wall) by wall roughness, indicating that the spanwise particle velocity fluctuations continue to be in local equilibrium with the local turbulent fluid flow as observed in the smooth-wall case for $St = 2.60$ and rough-wall cases for $St = 0.65$ (c.f., Figure 6).

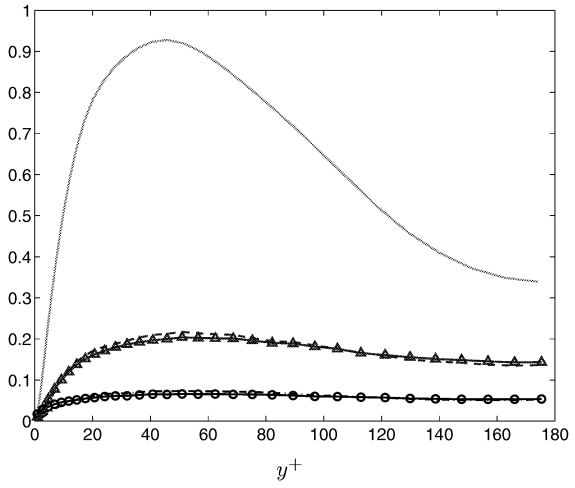

Figure 9: Influence of Stokes number on the spanwise velocity variance, $\gamma = 2.5°$. ——— fluid; △——△ $St = 0.65$; o——o $St = 2.60$; - - - - fluid-particle correlation for $St = 0.65$; —·— fluid-particle correlation for $St = 2.60$.

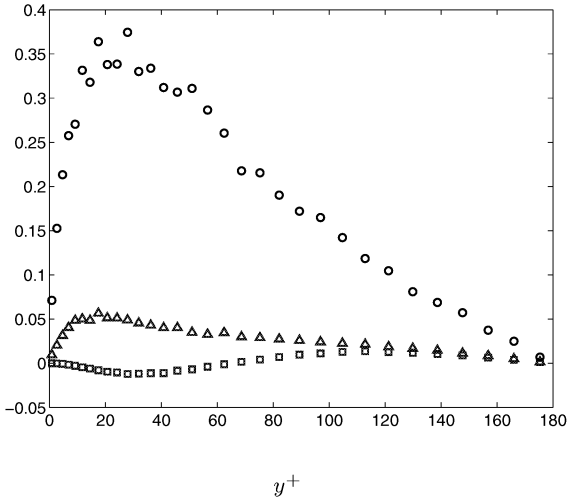

Figure 10: Influence of roughness on turbulent transport of the wall-normal particle velocity variance by the wall-normal particle velocity, $\langle v'_{p,2} v'_{p,2} v'_{p,2} \rangle_p$, $St = 0.65$. □ $\gamma' = 0°$; △ $\gamma' = 2.5°$; ○ $\gamma' = 5°$.

Turbulent transport

Figures 4-9 show that the largest effects on the particle fluctuating velocity occur in the wall-normal component and that for either increasing roughness or increasing Stokes number the velocity variance can be amplified throughout the channel, not only in the near-wall region close to the surface where roughness effects would be expected to be the most significant. Some insight into this effect is possible via examination of the triple velocity correlations. Shown in Figure 10 are profiles of the wall-normal turbulent transport of the wall-normal particle velocity variance, $\langle v'_{p,2} v'_{p,2} v'_{p,2} \rangle_p$. The wall-normal gradient of $\langle v'_{p,2} v'_{p,2} v'_{p,2} \rangle_p$ appears in the transport equation for the wall-normal velocity variance and therefore the behavior of the triple correlation should provide insight into the changes observed in the wall-normal velocity variance.

Figure 10 shows the effect of wall roughness on $\langle v'_{p,2} v'_{p,2} v'_{p,2} \rangle_p$ for $St = 0.65$. For the smooth-wall case, $\gamma' = 0°$, the triple correlation is small, which is expected given the good agreement shown previously between the particle wall-normal velocity variance and fluid-particle velocity correlation. Figure 10 also shows that with increases in the roughness angle there is a significant increase in $\langle v'_{p,2} v'_{p,2} v'_{p,2} \rangle_p$ with the increase from the wall to a peak value and the decrease to the core of the channel indicative of a transport of the wall-normal particle velocity variance from the near-wall region to the channel core.

SUMMARY AND PERSPECTIVES

The present effort focused on the influence of wall roughness on the transport characteristics of heavy particles in a gas-solid turbulent channel flow. The motion of the particles was dictated by their interactions with the local turbulent fluid flow and wall collisions. The smooth-wall cases show the effects characteristic of turbulent channel flow in the absence of particle-particle collisions or surface roughness, e.g., a peak in the near-wall particle number density and strong anisotropy of the particle velocity fluctuations. LES-DPS results for the smooth-wall case show the particle fluctuating motion in the wall-parallel directions is at equilibrium with the local turbulent flow, as evidenced by the good agreement between the particle velocity variance and corresponding component of the fluid-particle velocity correlation.

In general, while it would be anticipated that wall roughness will lead to direct changes to the particle velocities in the very near wall region, particle collisions with roughened surfaces can also lead to enhancements in particle transport across the entire channel. The current simulations show that the mean number density becomes more uniform as compared to the smooth-wall results, for cases with wall roughness and larger Stokes numbers. The mean streamwise velocity of the particles was also increased near the wall in the rough-wall cases.

For the particle fluctuating motion, wall roughness disrupts the equilibrium between the particle velocity fluctuations and local turbulent flow in the wall-normal direction, but not along the spanwise coordinate. LES-DPS results showed that the spanwise particle velocity variance was negligibly altered from the smooth-wall result in cases with wall roughness. Thus, the effect of wall roughness, as modeled in the present effort, does not result in nominally equivalent effects amongst the particle fluctuating velocities. Examination of the triple velocity correlation representing the wall-normal transport of the wall-normal particle velocity variance shows large changes with increasing roughness. Turbulent transport is important to increasing velocity fluctuations across the channel for the larger Stokes numbers and/or larger roughness angles.

REFERENCES

Kussin, J., and Sommerfeld, M., 2002, "Experimental studies on particle behavior and turbulence modification in horizontal channel flow with different wall roughness", *Exp. Fluids*, Vol. 33, pp. 143-159.

Laviéville, J., Simonin, O. and Deutsch, E., 1995, "Large Eddy Simulation of interactions between colliding particles and a homogeneous isotropic turbulence field", *Gas-Solid Flows*, ASME FED vol. 228, pp. 347-357.

Simonin, O., Deutsch, E. and Boivin, M., 1995, "Large eddy simulation and second-moment closure model of particle fluctuating motion in two-phase turbulent shear flows," in *Turbulent Shear Flow 9*, F. Durst, N. Kasagi, B.E. Launder, F.W. Schmidt, J.H. Whitelaw (eds.), Springer-Verlag (Heidelberg), pp. 85-115.

Sommerfeld, M., and Huber, N., 1999, "Experimental analysis and modelling of particle-wall collisions", *Int. J. Multiphase Flow*, Vol. 25, pp. 1457-1489.

Sommerfeld, M., 1992, "Modelling of particle-wall collisions in confined gas-particle flows", *Int. J. Multiphase Flow*, Vol. 18, pp. 905-926.

Sommerfeld, M., 2003, "Analysis of collision effects for turbulent gas-particle flow in a horizontal channel: Part I. Particle transport", *Int. J. Multiphase Flow*, Vol. 29, pp. 675-699.

Wang, Q. and Squires, K.D., 1996, "Large eddy simulation of particle-laden turbulent channel flows", *Phys. Fluids*, **8**, pp. 1207-1223.

Yamamoto, Y., Potthoff, M., Tanaka, T., Kajishima, T. and Tsujui, T., 2001, "Large-eddy simulation of turbulent gas-particle flow in a vertical channel: effect of considering inter-particle collisions", *J. Fluid Mech.*, Vol. 442, pp. 303-334.